

See discussions, stats, and author profiles for this publication at: <https://www.researchgate.net/publication/264165004>

# Dualsteric Muscarinic Antagonists–Orthosteric Binding Pose Controls Allosteric Subtype Selectivity

ARTICLE in JOURNAL OF MEDICINAL CHEMISTRY · JULY 2014

Impact Factor: 5.45 · DOI: 10.1021/jm500790x · Source: PubMed

---

CITATIONS

5

READS

271

---

## 10 AUTHORS, INCLUDING:



[Marcel Bermudez](#)

Freie Universität Berlin

10 PUBLICATIONS 49 CITATIONS

[SEE PROFILE](#)



[Jessica Kloeckner](#)

Catalent, Inc

11 PUBLICATIONS 101 CITATIONS

[SEE PROFILE](#)



[Evi Kostenis](#)

University of Bonn

144 PUBLICATIONS 4,901 CITATIONS

[SEE PROFILE](#)



[Gerhard Wolber](#)

Freie Universität Berlin

148 PUBLICATIONS 2,853 CITATIONS

[SEE PROFILE](#)

## Dualsteric Muscarinic Antagonists—Orthosteric Binding Pose Controls Allosteric Subtype Selectivity

Jens Schmitz,<sup>†</sup> Dorina van der Mey,<sup>‡</sup> Marcel Bermudez,<sup>§</sup> Jessica Klöckner,<sup>†</sup> Ramona Schrage,<sup>‡</sup> Evi Kostenis,<sup>||</sup> Christian Tränkle,<sup>‡</sup> Gerhard Wolber,<sup>§</sup> Klaus Mohr,<sup>\*,‡</sup> and Ulrike Holzgrabe<sup>\*,†</sup>

<sup>†</sup>Institute of Pharmacy and Food Chemistry, University of Würzburg, Am Hubland, D-97074 Würzburg, Germany

<sup>‡</sup>Pharmacology and Toxicology, Institute of Pharmacy, Gerhard-Domagk-Straße 3, D-53121 Bonn, Germany

<sup>§</sup>Institute for Pharmacy, Free University Berlin, Königin-Luise-Straße 2 und 4, D-14195 Berlin, Germany

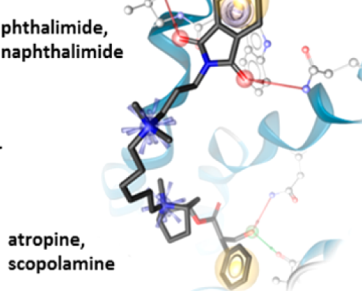
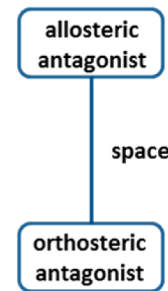
<sup>||</sup>Institute of Pharmaceutical Biology, Molecular-, Cellular-, and Pharmacobiology Section, University of Bonn, Nussallee 6, D-53115 Bonn, Germany

### Supporting Information

**ABSTRACT:** Bivalent ligands of G protein-coupled receptors have been shown to simultaneously either bind to two adjacent receptors or to bridge different parts of one receptor protein. Recently, we found that bivalent agonists of muscarinic receptors can simultaneously occupy both the orthosteric transmitter binding site and the allosteric vestibule of the receptor protein. Such dualsteric agonists display a certain extent of subtype selectivity, generate pathway-specific signaling, and in addition may allow for designed partial agonism. Here, we want to extend the concept to bivalent antagonism. Using the phthal- and naphthalimide moieties, which bind to the allosteric, extracellular site, and atropine or scopolamine as orthosteric building blocks, both connected by a hexamethonium linker, we were able to prove a bitopic binding mode of antagonist hybrids for the first time.

This is demonstrated by structure–activity relationships, site-directed mutagenesis, molecular docking studies, and molecular dynamics simulations. Findings revealed that a difference in spatial orientation of the orthosteric tropane moiety translates into a divergent M<sub>2</sub>/M<sub>5</sub> subtype selectivity of the corresponding bitopic hybrids.

### dualsteric antagonists:



### INTRODUCTION

The superfamily of G protein-coupled receptors (GPCRs) consists of more than 800 members mediating responses of messenger compounds such as neurotransmitters and hormones as well as physical stimuli such as light.<sup>1</sup> The structures of all GPCRs being integral membrane proteins have in common an extracellular domain (ECD) for stimulus recognition, a seven transmembrane (7TM) helical protein-fold, and an intracellular domain (ICD) for signal propagation to transducers such as G proteins. The recently published X-ray structures of class A GPCRs, e.g., β<sub>1</sub>- and β<sub>2</sub>-adrenergic receptors,<sup>2</sup> as well as A<sub>2A</sub> adenosine,<sup>3</sup> dopamine D<sub>3</sub>,<sup>4,5</sup> histamine H1,<sup>6</sup> and muscarinic M<sub>2</sub><sup>7,8</sup> and M<sub>3</sub><sup>9</sup> receptors show similar motifs of the orthosteric, endogenous activator binding site, whereas the entrance of the ligand binding cavity is structurally diverse. The ECD forms a vestibule which appears to be critical for activation-related conformational rearrangement of the receptor protein.<sup>8,10</sup> In addition, water molecules are removed from the orthosteric ligand on its way through the vestibule.<sup>11,12</sup>

The structural diversity of the ECD region between receptor subtypes is attractive from a medicinal chemistry point of view as the ECD may be exploited to gain selective action. Such

allosteric ligands may induce agonism with corresponding downstream signaling even though they do not bind to the orthosteric pocket. In addition, an allosteric ligand may form a ternary complex with an orthosteric agonist-bound receptor, resulting in a modulation of the binding and the signaling of the orthoster.<sup>13</sup>

Alternatively, alloster and orthoster can be combined within one molecule. We recently designed an M<sub>2</sub>-preferring hybrid compound<sup>14,15</sup> consisting of the orthosteric superagonist iperoxo (“iper”),<sup>16</sup> which activates all subtypes of the muscarinic receptor,<sup>17,18</sup> and a subtype-selective allosteric ligand (i.e., either a phthalimido- or a naphthalimido-propylamino moiety (“phth” and “naph”, respectively)). Both pharmacophores were linked by a hexamethonium chain (see Figure 1). These hybrids bind in a dualsteric fashion, i.e., simultaneous allosteric/orthosteric binding, and generate pathway-specific (biased) signaling.<sup>10</sup> It is worth noting that some of these dualsteric derivatives recently showed interesting analgesic properties in *in vivo* experiments.<sup>19</sup> Bitopic allosteric/orthosteric binding was reported for the M<sub>2</sub> receptor also by

Received: May 21, 2014

Published: July 22, 2014



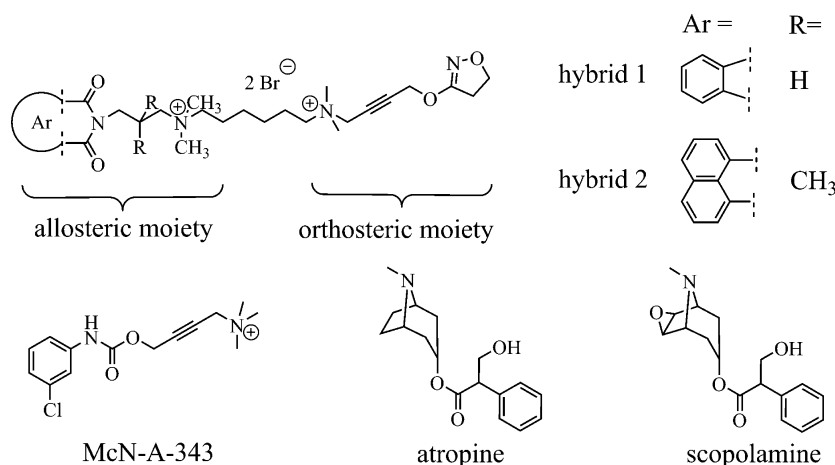


**Figure 1.** Structural formulas of hybrid 1 and 2 consisting of the allosteric and the orthosteric part connected via a hexamethylene linker, McN-A-343, atropine, and scopolamine.

Valant et al. for McN-A-343<sup>20</sup> (see Figure 1) and for the M<sub>1</sub> receptor.<sup>21–23</sup> Yet, a bivalent design does not necessarily imply bitopic binding. Instead of “diving down” with its orthosteric head into the depth of the receptor’s ligand binding cavity, the bivalent compound may prefer purely allosteric binding. In this pose, the orthosteric head is directed toward the extracellular surface of the receptor, thus not contributing to binding and action.<sup>15</sup> The probability of poses depends on the ratio of respective binding affinities. This “dynamic ligand binding” has recently been exploited to achieve designed partial agonism.<sup>24</sup>

The muscarinic M<sub>2</sub> receptor is archetypal for the investigation of allosteric GPCR interactions.<sup>25-27</sup> Yet, designed dualsteric antagonism has not been reported so far. As activation of the M<sub>2</sub> receptor involves a major conformational transition including the allosteric binding area,<sup>8,10</sup> we set out to check whether the dualsteric design concept for active receptors can be translated to the inactive M<sub>2</sub> receptor. To this end, we employed the same allosteric motif (see Figure 1) and linker as with the aforementioned hybrid agonists, but replaced their orthosteric agonist moiety, i.e., the superagonist iperoxo,<sup>16</sup> with the inverse agonist moieties atropine and scopolamine, respectively. Putative binding mode and subtype selectivity were elucidated by using wild-type M<sub>2</sub> as well as receptor mutants of the orthosteric and allosteric site.<sup>28,29</sup> Additionally, the binding mode was checked by docking and molecular dynamics simulations, and antagonism was assessed real-time by a label-free whole cell assay. The findings reveal that the inactive receptor state allows for the binding of orthosteric/allosteric hybrid molecules. However, only the appropriate choice of the orthosteric portion may induce a fruitful anchoring of the allosteric counterpart, thus exploiting the potential subtype selectivity of the resulting dualsteric molecular probe.

## ■ RESULTS AND DISCUSSION

**Chemistry.** To obtain allosteric/orthosteric hybrid compounds as antagonists for muscarinic receptors, an allosteric phthalimide moiety has to be connected to an orthosteric moiety, i.e., atropine and scopolamine, respectively. The alloster skeleton synthesis starts off with the conversion of phthalic and naphthalic anhydride, respectively, with the corresponding *N,N'*-dimethyl-1,3-propanediamine and a catalytic amount of *p*-toluenesulfonic acid by means of a microwave heating (cf. ref.

30–32). The resulting amines **1** and **2**, respectively, were refluxed with an excess of 1,6-dibromohexane (no solvent!) to achieve the monoammonium salts **3** and **4** (Scheme 1).<sup>30,32</sup> Finally, a nucleophilic substitution of the halogen with the amino function of atropine and scopolamine, respectively, leads to the twice positively charged hybrids **5–8**. The latter reaction lasts days to weeks and cannot be speeded up by microwave application. Along these lines, the shortened hybrids **9** and **10** were synthesized by heating atropine and scopolamine, respectively, with *N'*-bromohexyl-*N,N,N*-trimethylammonium bromide obtained from the conversion of trimethylammonium choride with dibromohexane.<sup>15</sup>

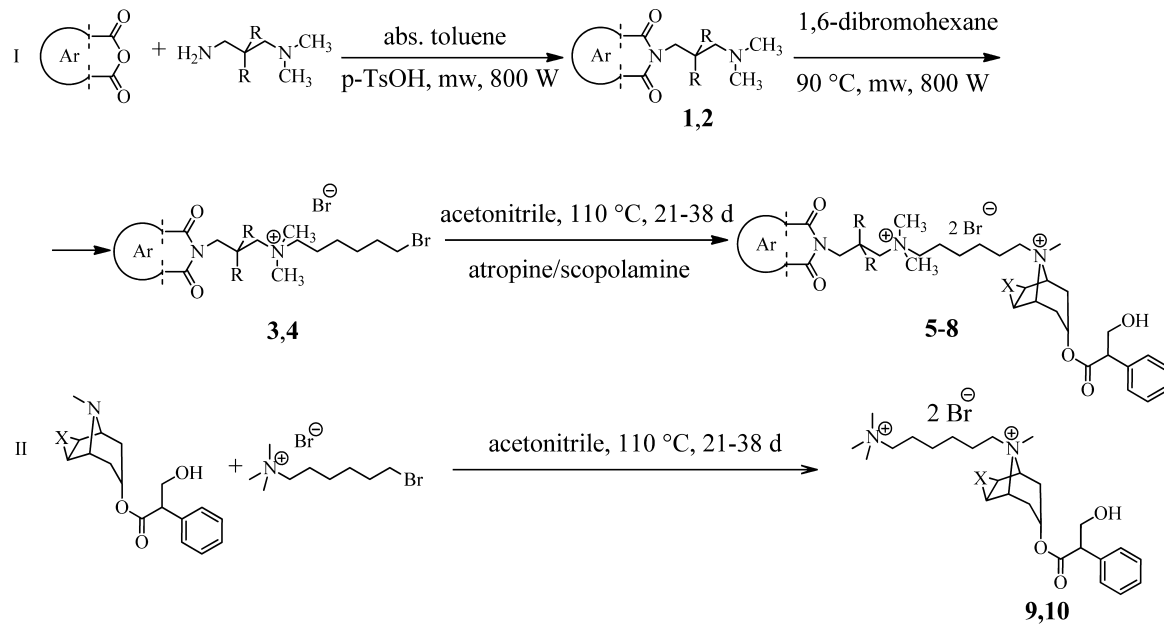
**Stereochemistry.** Tropane alkaloids are known to undergo epimerization via inversion at the nitrogen atom in solution. Hence, the methyl group can take either an *anti* or an *syn* position.<sup>33</sup> By means of  $^{13}\text{C}$  NMR spectroscopy, the two diastereomers can be distinguished by recording the spectra at low temperatures ( $-70\text{ }^\circ\text{C}$ ), which increases the lifetime of the epimers,<sup>34</sup> e.g., the diastereomers of tropine free base, a building block of atropine and scopolamine, showed a 20-fold higher preference of the *anti* position of the methyl group.

For binding/docking of the orthosteric part to the receptor binding pocket, it is pivotal to know whether the linker takes an *syn* or *anti* position at the tropine skeleton. Therefore, NOESY experiments were performed utilizing the nuclear Overhauser effect NOE between the *N*-methyl and the tropine protons. Because of a mutual enhancement of the *N*-methyl hydrogens and the *exo* tropine protons at C-2 and C-4, it can be deduced that the products predominantly bear the methyl group in *syn* and the more voluminous linker moiety in *anti* position.

The synthesis of the corresponding agonist hybrid molecules was already described by Antony et al.<sup>15</sup> and Bock et al.<sup>10</sup> (Figure 2).

**Structure–Binding Relationships Suggested Duals-teric Binding.** Test compound binding was measured in membranes from CHO cells stably transfected with cDNA encoding for the human muscarinic M<sub>2</sub> receptor. The radiolabeled orthosteric inverse agonist [<sup>3</sup>H]-N-methylscopolamine ([<sup>3</sup>H]NMS) was used to explore test compound binding under equilibrium conditions (Figure 3, open columns). Furthermore, inhibition of [<sup>3</sup>H]NMS dissociation by the test compounds revealed ternary complex formation, i.e., purely allosteric test compound binding to the [<sup>3</sup>H]NMS-occupied receptor (Figure 3, filled columns).

Scheme 1. Synthesis Pathway for Antagonist-Allosteric Hybrids



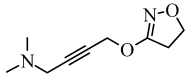
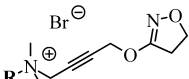
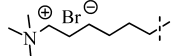
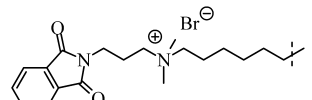
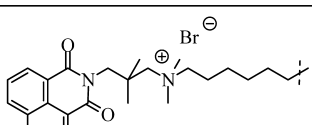
compound	R	-X-	antagonist	allosteric moiety	name
<b>5</b>	H	-	atropine	phthalimide	Atr-6-phth
<b>6</b>	CH <sub>3</sub>	-	atropine	naphthalimide	Atr-6-naph
<b>7</b>	H	O	scopolamine	phthalimide	Sco-6-phth
<b>8</b>	CH <sub>3</sub>	O	scopolamine	naphthalimide	Sco-6-naph
<b>9</b>	-	-	atropine	N'-hexyl-N,N,N-trimethylammonium bromide	Atr-6
<b>10</b>	-	O	scopolamine	N'-hexyl-N,N,N-trimethylammonium bromide	Sco-6

Each of the two *allosteric* parent compounds, i.e., W84 and naphmethonium, displayed similar affinity for both the free and the orthostERICALLY [<sup>3</sup>H]NMS-bound hM<sub>2</sub> receptor (Figure 3, open and filled columns, respectively). This is in line with previous findings showing that these agents are pure allosteric binders in both the orthostERICALLY free and the NMS-bound M<sub>2</sub> receptor.<sup>35</sup>

In contrast, the *orthosteric* parent compounds atropine, scopolamine, and their respective derivatives had much higher affinity for the free M<sub>2</sub> receptor (Figure 3, open columns) compared with the M<sub>2</sub> receptor orthostERICALLY blocked by [<sup>3</sup>H]NMS (Figure 3, filled columns). The same applied to both series of bivalent antagonists (atropine-containing compounds Atr-6-phth (**5**), Atr-6-naph (**6**), and Atr-6 (**9**), and scopolamine-containing compounds Sco-6-phth (**7**), Sco-6-naph (**8**), and Sco-6 (**10**)) as well as to their agonistic counterparts

(iperoxo-containing compounds Iper-6 (**13**), Iper-6-phth (**14**), and Iper-6-naph (**15**)).

Regarding structure–binding relationships for the *free hM2 receptor* (Figure 3, open columns), N-methylation of orthostERIC compounds (atropine, scopolamine, desmethyl-iper (**11**)) increased affinity in all series of compounds (MAtr, MSco, iper (**12**)). Further elongation of the substituent by the trimethylammonium-hexyl linker (yielding Atr-6 (**9**), Sco-6 (**10**), and iper-6 (**13**)) reduced binding affinity in each series of compounds, but to a different extent: relative to the orthostERIC parent compounds (i.e., atropine, scopolamine, desmethyl-iper (**11**)), the respective affinity of their congeners (**9**, **10**, **13**) was lowered in the case of the antagonists (**9**, **10**) but not in the case of the agonist (**13**). The latter finding may result from the agonist-induced activation-dependent spatial rearrangement of the allosteric vestibule.<sup>10,36</sup> Further elongation of the allosteric building block by either a phthalimide residue or the

compound		name
11		desmethyl-iper
		
R:		
12	$\text{H}_3\text{C}^+$	iper
13		iper-6
14		iper-6-phth
15		iper-6-naph

**Figure 2.** Structural formulas of the agonist related compounds 11–15.

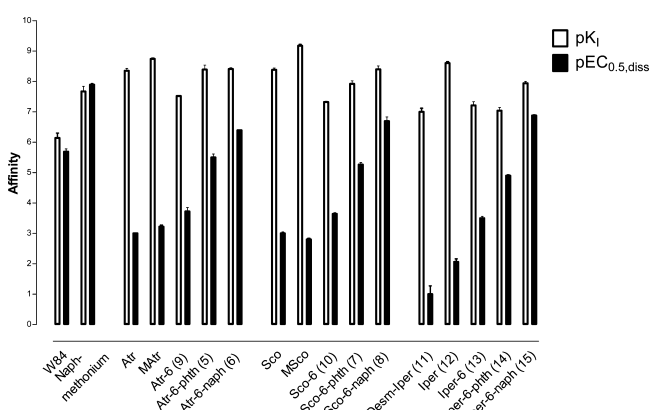


**Figure 3.** Orthosteric and allosteric test compound binding at the M<sub>2</sub> receptor. Ordinate: minus log-binding constant for the free ( $pK_d$ , open columns) and the orthostERICALLY blocked receptor ( $pEC_{0.5,\text{diss}}$ , filled columns: concentration for a half-maximum inhibition of [<sup>3</sup>H]NMS-dissociation). Abscissa: test compounds. Shown are mean values  $\pm$  SEM from 3 to 11 individual determinations.

corresponding naphthalimide moiety increased affinity of the antagonist hybrids (Atr-6-phth (5), Sco-6-phth (7)), indicating additional exploitation of the allosteric site. In the series of receptor activators, elongation by the naph- but not by the phth-moiety enhanced affinity.

Regarding purely allosteric interactions at the [<sup>3</sup>H]NMS-bound M<sub>2</sub> receptor (filled columns in Figure 3), the very low affinity of the orthostERIC parent compounds revealed poor complementarity with the allosteric site. Allosteric affinity was increased upon introduction of the linker chain and was even further elevated upon introduction of an allosteric building block. Yet, affinity of the hybrids for the [<sup>3</sup>H]NMS-bound M<sub>2</sub> receptor

clearly fell behind the affinity attained at the [<sup>3</sup>H]NMS-free receptor.

In conclusion, fusion of systematically enlarged allosteric residues to orthostERIC ligands modulated affinity following a pattern that was similar between bivalent antagonists and agonists. In case of the latter, a dualsteric (allosteric/orthostERIC) binding topography had been validated in the past applying various strategies.<sup>10,13,15,20,37–39</sup> Therefore, the parallel structure–activity relationships between the novel bivalent antagonists and the established bivalent agonists suggested that bivalent hybrid antagonists attach to the muscarinic M<sub>2</sub> receptor in the bitopic allosteric/orthostERIC mode.

#### An OrthostERIC Mutation Revealed Dualsteric Binding.

The epitope hM2-Y104<sup>3,33</sup> is located in the orthostERIC site next to the core amino acid hM2-D103 (hM<sub>2</sub>-Y104<sup>3,33</sup>A according to the Ballesteros and Weinstein nomenclature<sup>40</sup>). The latter is crucial as a docking point for the cationic headgroup of acetylcholine and related orthostERIC agonists and antagonists (e.g., Kruse et al.<sup>8</sup>). Mutation of the adjacent M<sub>2</sub> Y104<sup>3,33</sup> to A diminished orthostERIC ligand affinity considerably, yet leaving sufficient affinity for the orthostERIC probe [<sup>3</sup>H]N-methylscopolamine to be employed as an orthostERIC probe,<sup>15</sup> ([<sup>3</sup>H]NMS  $K_D$  values: M<sub>2</sub> wt  $9.37 \pm 0.04$ ,  $n = 22$  vs M<sub>2</sub> Y104<sup>3,33</sup>A,  $7.98 \pm 0.05$ ,  $n = 20$ ). M<sub>2</sub> Y104<sup>3,33</sup> has also been shown to contribute to the binding of muscarinic superagonists such as iperoxo<sup>16</sup> and to the binding of iper-derived dualsteric agonists such as iper-6-phth (14) and iper-6-naph (15).<sup>15</sup> In the present study, mutation of M<sub>2</sub> Y104<sup>3,33</sup> to A induced a significant fall of binding affinity in the case of all applied orthostERIC test compounds (Figure 4, Table 1). In contrast, and as expected, the affinities of the allosteric ligands W84 and naphmethonium were insensitive to the orthostERIC mutation (Table 1).

Taken together, findings with the orthostERIC M<sub>2</sub> Y104<sup>3,33</sup>A mutant confirmed interaction with the orthostERIC binding site for all tested ortho-/allosteric antagonists.

#### Hybrid-Dependent Differential Sensitivity to Allosteric Receptor Mutagenesis.

Archetypal bis-ammonio-alkane-type muscarinic allosteric modulators are subtype selective with highest affinity for the M<sub>2</sub> subtype and lowest for M<sub>5</sub>.<sup>28,41,42</sup> The epitopes M<sub>2</sub> Y177<sup>EL2</sup> of the second extracellular loop as well as M<sub>2</sub> T423<sup>7,36</sup> at the beginning of transmembrane helix 7 were found to be critical for allosteric subtype selectivity.<sup>28</sup> M<sub>2</sub>-W422<sup>7,35</sup> is conserved among the five muscarinic receptor subtypes and involved in allosteric baseline affinity as well as in orthostERIC ligand-induced receptor activation.<sup>10,29,36</sup>

In contrast to the allosteric building blocks W84 and naphmethonium, none of their antagonist derivatives was sensitive to the M<sub>2</sub>/M<sub>5</sub>-double mutant M<sub>2</sub> Y177<sup>EL2</sup>Q + T423<sup>7,36</sup>H (Table 1). The single point mutant M<sub>2</sub> Y177<sup>EL2</sup>Q, however, disclosed a significant contribution of the allosteric M<sub>2</sub> Y177<sup>EL2</sup> for the affinity of the atropine-derived hybrids Atr-6-phth (5) and Atr-6-naph (6) (Table 1). The binding affinity of the scopolamine-derived hybrids Sco-6-phth (7) and Sco-6-naph (8) was independent of M<sub>2</sub> Y177<sup>EL2</sup>. In line with this, the affinity of the hybrids Atr-6-phth (5) and Atr-6-naph (6) for the M<sub>5</sub> subtype, containing Q instead of Y in position 177<sup>EL2</sup>, was significantly lower compared with their affinity for the M<sub>2</sub> subtype, whereas the corresponding scopolamine-derived hybrids Sco-6-phth (7) and Sco-6-naph (8) did not discriminate between the M<sub>2</sub> and the M<sub>5</sub> subtype (Table 1).

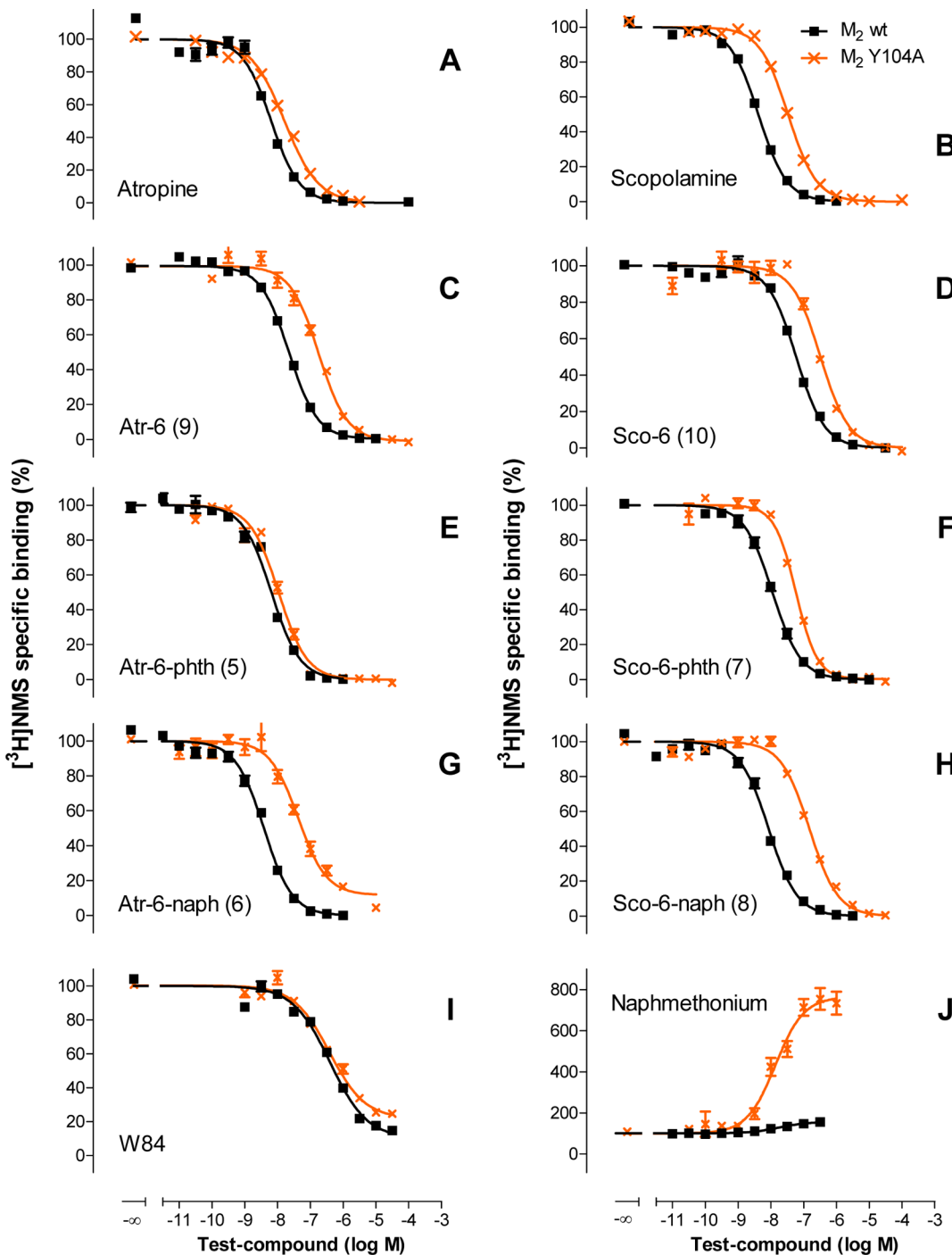


**Figure 4.** Role of an orthosteric key epitope for test compound-binding. Shown is test compound-induced inhibition of the binding of the orthosteric antagonist probe  $[^3\text{H}]$ N-methylscopolamine from the wild-type  $M_2$  (black) and the orthosteric mutant  $M_2$  Y104A (red) in membranes of FlpIn-CHO cells stably transfected with the respective receptor gene: (A,B) orthosteric antagonists; (C,D) linker chain-containing intermediates; (E–H) antagonistic hybrids; (I,J) purely allosteric ligands. Ordinate: Specific binding of  $[^3\text{H}]$ NMS ( $M_2$  wt, 0.2 nM;  $M_2$  Y104A, 1.0 nM) in percent of  $[^3\text{H}]$ NMS-binding in the absence of test compound. Abscissa: log concentration of test compound. Curves were obtained by nonlinear regression analysis applying (A–H) a four parameter logistic equation or (I,J) the allosteric ternary complex model. Given are means  $\pm$  SEM of 3–4 independent experiments performed as triplicate determinations.

Regarding the conserved allosteric/orthosteric interface epitope  $M_2$ -W422<sup>7,35</sup>, the corresponding mutant  $M_2$ -W422<sup>7,35</sup>A, (7.35 according to Ballesteros and Weinstein)<sup>29</sup> revealed that the affinities of the atropine-derived hybrids Atr-6 (9), Atr-6-phth (5), and Atr-6-naph (6) were significantly diminished by mutation of this epitope (Table 1). In the case of the corresponding scopolamine-derived hybrids, however,

neither the affinity of the parent compound scopolamine nor the affinities of Sco-6 (10), Sco-6-phth (7), nor Sco-6-naph (8) were affected by the mutation.

Taken together, findings suggested that the type of orthosteric building block was critical for an exploitation of allosteric  $M_2/M_5$  selectivity by a dualsteric antagonist.

Table 1. Binding Affinity Estimates of the Indicated Test Compounds at the Indicated Receptors<sup>a</sup>

	M <sub>2</sub> wt	M <sub>2</sub> Y104A	M <sub>2</sub> Y177Q	M <sub>2</sub> Y177Q T423H	M <sub>2</sub> W422A	M <sub>5</sub> wt
<b>Atropine</b>	8.30 ± 0.08 (3)	7.89 ± 0.09 * (4)	8.44 ± 0.04 (3)	8.34 ± 0.05 (3)	8.55 ± 0.03 * (4)	8.52 ± 0.10 (6) n.d.
<b>MAtr</b>	8.74 ± 0.03 (3)	7.96 ± 0.08 * (4)	n.d.	n.d.	n.d.	n.d.
<b>Atr-6 (9)</b>	7.79 ± 0.05 (4)	6.82 ± 0.06 * (4)	7.73 ± 0.03 (3)	7.74 ± 0.04 (3)	7.26 ± 0.05 * (4)	7.06 ± 0.04 (3)
<b>Atr-6-phth (5)</b>	8.28 ± 0.07 (3)	8.01 ± 0.07 * (5)	8.01 ± 0.01 * (3)	8.27 ± 0.04 (3)	7.78 ± 0.10 * (4)	7.78 ± 0.10 * (4)
<b>Atr-6-naph (6)</b>	8.55 ± 0.02 (3)	7.21 ± 0.06 * (4)	8.07 ± 0.06 * (3)	8.55 ± 0.07 (4)	7.67 ± 0.08 * (4)	7.71 ± 0.03 * (4)
<b>Scopolamine</b>	8.52 ± 0.05 (3)	7.54 ± 0.06 * (3)	8.48 ± 0.07 (3)	8.45 ± 0.02 (3)	8.48 ± 0.08 (3)	8.89 ± 0.07 * (4)
<b>MSco</b>	9.37 ± 0.04 (22)	7.98 ± 0.05 * (20)	9.14 ± 0.06 * (8)	9.48 ± 0.06 (7)	9.36 ± 0.04 (3)	8.95 ± 0.08 * (3)
<b>Sco-6 (10)</b>	7.32 ± 0.03 (3)	6.51 ± 0.03 * (4)	n.d.	n.d.	7.39 ± 0.04 (3)	7.68 ± 0.06 * (4)
<b>Sco-6-phth (7)</b>	8.09 ± 0.12 (3)	7.30 ± 0.05 * (4)	8.15 ± 0.04 (4)	8.15 ± 0.03 (3)	8.16 ± 0.06 (4)	7.77 ± 0.08 (3)
<b>Sco-6-naph (8)</b>	8.21 ± 0.08 (7)	6.88 ± 0.04 * (5)	8.05 ± 0.03 (3)	8.48 ± 0.01 (3)	8.19 ± 0.08 (3)	8.26 ± 0.08 (4)
<b>Desm-Iper (11)</b>	7.00 ± 0.12					
<b>Iper (12)</b>	8.60 ± 0.05 (4)	6.59 ± 0.07 * (4)	8.06 ± 0.13 * (4)	8.66 ± 0.06 (4)	8.00 ± 0.09 * (4)	6.92 ± 0.06 * (3)
<b>Iper-6 (13)</b>	7.21 ± 0.12 (4)	5.89 ± 0.04 * (3)	7.04 ± 0.12 (6)	7.19 ± 0.05 (3)	6.56 ± 0.16 * (4)	5.40 ± 0.13 * (3)
<b>Iper-6-phth (14)</b>	7.04 ± 0.10 (4)	6.69 ± 0.05 * (3)	6.56 ± 0.07 * (3)	6.70 ± 0.09 * (4)	7.12 ± 0.05 (3)	4.52 ± 0.09 * (3)
<b>Iper-6-naph (15)</b>	7.94 ± 0.06 (3)	7.84 ± 0.11 (3)	n.d.	7.57 ± 0.02 * (3)	7.71 ± 0.09 (4)	n.d.
<b>W84</b>	6.55 ± 0.03 (3)	6.59 ± 0.04 (3)	n.d.	5.47 ± 0.11 * (4)	n.d.	4.37 ± 0.09 * (5)
<b>Naphmethonium</b>	7.70 ± 0.12 (6)	7.64 ± 0.08 (5)	6.23 ± 0.07 * (3)	5.82 ± 0.06 * (5)	n.d.	5.05 ± 0.06 * (3)

<sup>a</sup>Listed are means ± SEM obtained by nonlinear regression analysis with a logistic equation followed by a Cheng–Prusoff correction ( $pK = -\log K_b$ , equilibrium inhibition constant) or by means of the allosteric ternary complex model according to Ehlert (1988;  $pK_A$ ) in case of W84 and naphmethonium. The number of experiments carried out as triplicate determinations is given in parentheses. \*, Statistically different from wild type M<sub>2</sub>, *t* test, *P* < 0.05.

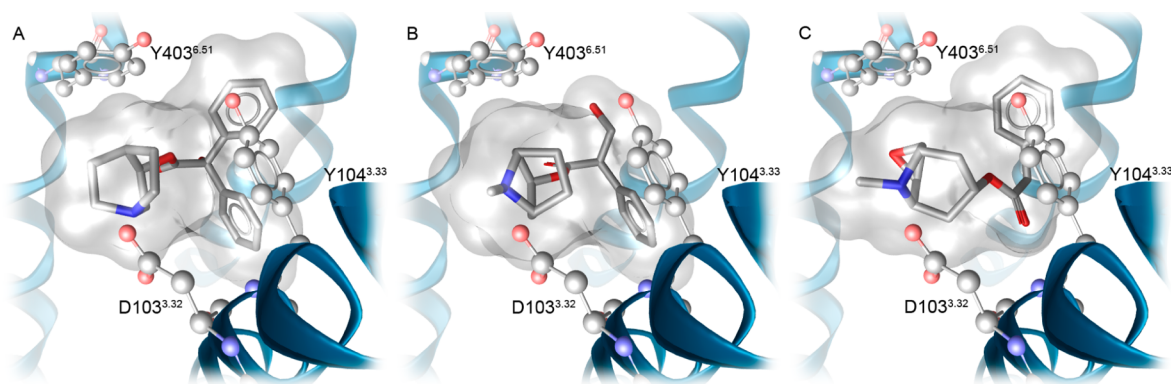
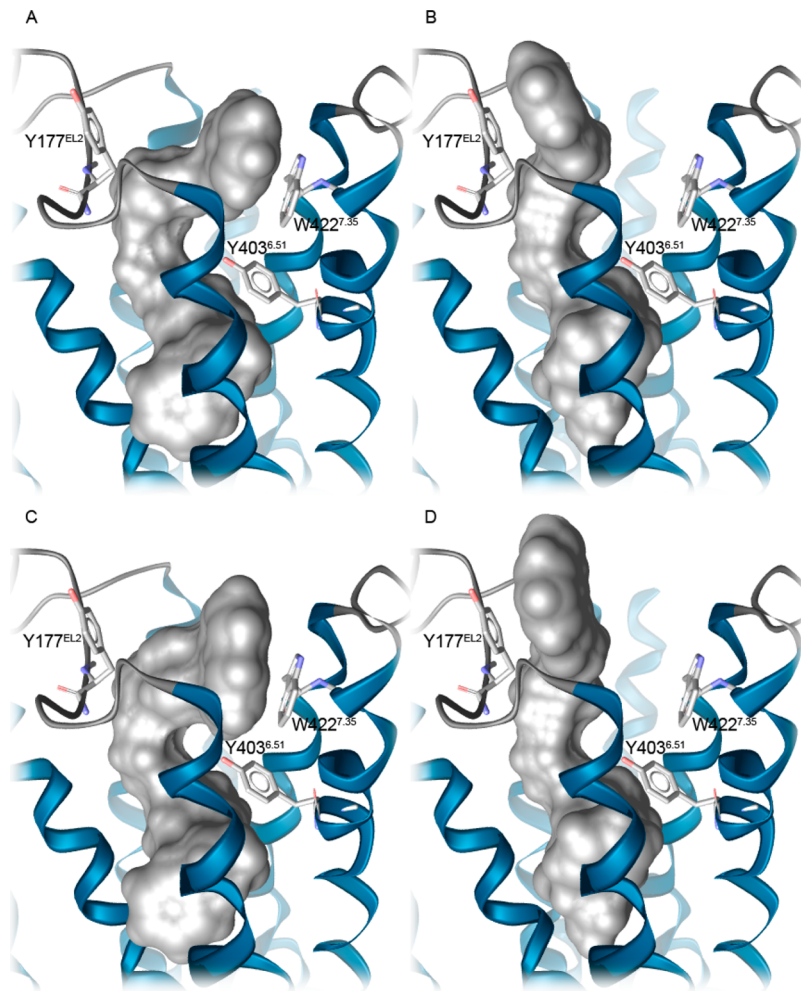


Figure 5. Comparison of the orientation of the orthosteric ligands (A) QNB, (B) atropine, and (C) scopolamine in the M<sub>2</sub> muscarinic acetylcholine receptor.

**Docking Studies and Molecular Dynamic Simulations Revealed Different Binding Poses of Orthosteric Building Blocks.** The crystal structure (PDB 3UON) of the M<sub>2</sub> receptor with cocrystallized orthosteric inverse agonist QNB offers insight into the orthosteric binding site, which mainly consists of aromatic residues (Figure 5).<sup>7</sup> M<sub>2</sub> Y104<sup>3.33</sup> and M<sub>2</sub> Y403<sup>6.51</sup> limit the orthosteric binding pocket toward the extracellular region, where the allosteric binding pocket is located. In the docking, the general ligand orientation was induced by an electronic interaction between M<sub>2</sub>-D103<sup>3.32</sup> and the respective quaternary nitrogen of QNB, atropine, and scopolamine. Opposite to this hydrophilic region there are two

lipophilic pockets. While QNB simultaneously fills both pockets with its two phenyl rings, docking revealed atropine and scopolamine to enter only one cavity each, interestingly not the same (Figure 5). The respective preference of the phenyl ring for one of these pockets was caused by the orientation of the tropane ring system. The required space of the epoxide group in scopolamine forced the tropane ring system into a different orientation compared with atropine. In addition, the epoxide appeared likely to form a hydrogen bond to the thiol group of C429<sup>7.42</sup> (not shown). This difference in tropane orientation resulted in two distinct binding modes for the respective allosteric building blocks: whereas the atropine-based hybrids



**Figure 6.** Molecular surfaces of (A) Atr-6-phth (**5**), (B) Sco-6-phth (**7**), (C) Atr-6-naph (**6**), and (D) Sco-6-naph (**8**) in the M<sub>2</sub> muscarinic acetylcholine receptor indicate a different arrangement of the allosteric part of atropine-based (A,C) and scopolamine-based hybrid structures (B,D).

appeared to directly interact with W422<sup>7.35</sup> (Figure 6A,C), the scopolamine-based hybrid structures turned out to be engaged with Y177<sup>EL2</sup> of extracellular loop 2 (Figure 6B,D). In fact, as found in the above-mentioned mutagenesis studies, atropine-based hybrids Atr-6-phth (**5**) and Atr-6-naph (**6**) were sensitive to the mutant M<sub>2</sub> W422<sup>7.35</sup>A, whereas binding of the corresponding scopolamine-based hybrids remained unaffected (cf. Table 1).

Instead, the model predicts epitope 177 in the extracellular loop 2 to play a key role for the binding of the scopolamine-based hybrids in both the M<sub>2</sub> and the M<sub>5</sub> receptor. Whereas M<sub>2</sub> Y177<sup>EL2</sup> hosts the allosteric ring systems through  $\pi-\pi$  interactions and hydrophobic contacts, M<sub>5</sub> Q177<sup>EL2</sup> is able to form a hydrogen bond to the carbonyl group of the allosteric ring system. This would explain why the scopolamine-based dualsteric ligands did not show M<sub>2</sub>/M<sub>5</sub> subtype selectivity. In contrast, the atropine-based dualsteric ligands significantly lost affinity in the M<sub>2</sub> Y177<sup>EL2</sup>Q mutant relative to wild-type M<sub>2</sub> (cf. Table 1).

Extensive molecular dynamics simulations of dualsteric structures Atr-6-phth (**5**), Atr-6-naph (**6**), Sco-6-phth (**7**), and Sco-6-naph (**8**) confirmed the difference in binding pose between the respective atropine-based and scopolamine-based hybrid structures. The main orientation of the allosteric part in the extracellular vestibule remained stable during 20 ns of

simulation time. Because of the constitutive activity of GPCRs, the distance between the allosteric epitopes Y177<sup>EL2</sup> and W422<sup>7.35</sup> highly varies in the simulation of the apo-structure, whereas it varies less in the simulations containing the hybrid structures bound to the protein. This reflects that dualsteric binding stabilizes the inactive receptor conformation. Details for the MD simulations can be found in the Supporting Information.

**Antagonistic Action of the Dualsteric Ligands.** The expected muscarinic antagonistic action of the hybrid antagonists was investigated by employing cellular dynamic mass redistribution (DMR) as the read-out. Atr-6-naph (**6**) was employed as a representative dualsteric ligand. Addition of acetylcholine in a maximally effective concentration to hM2-CHO cells induced a brisk positive DMR signal (Figure 7). The signal was reversed by addition of the orthosteric antagonist atropine, the allosteric naphmethonium, and the hybrid Atr-6-naph (**6**) (Figure 7, upper, middle, and lower panel, respectively). Worth mentioning, the dualsteric antagonist at the highest applied concentration of 100  $\mu$ M did not have any nonspecific action in the absence of atropine (data not shown). The action of Atr-6-naph (**6**) was not delayed relative to that of atropine and naphmethonium. Most probably the onset of antagonist action is diffusion limited and does not reflect true ligand association. Nevertheless, traces induced by Atr-6-naph

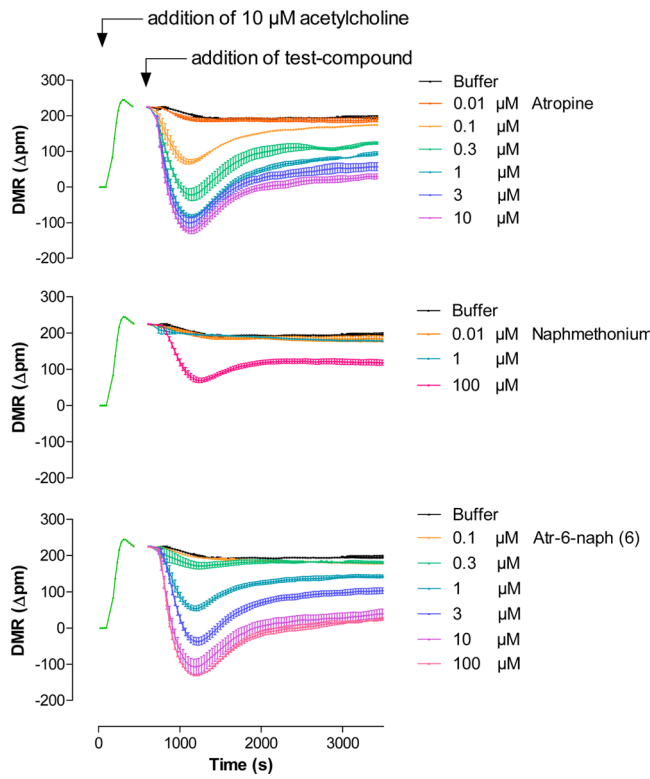


**Figure 7.** Time-course of antagonist action in living hM<sub>2</sub>-CHO cells. Cellular dynamic mass redistribution (ordinate: DMR, wavelength shift in pm) was initiated by addition of acetylcholine. Reversal of acetylcholine action was checked by addition of indicated test-compounds: orthosteric atropine, allosteric naphmethonium, dualsteric Atr-6-naph (**6**) at the indicated concentrations. Shown is a representative experiment (mean values  $\pm$  SEM,  $n = 4$ ) that was repeated at least twice on separate days (Hank's Balanced Salt Solution, HBSS, supplemented with 20 mM HEPES, pH 7).

(6) suggest that binding in the bitopic pose does not go along with a gross reduction of the probability of association to and dissociation from the ligand binding pocket.

## CONCLUSION

Previously, bivalent orthosteric/allosteric activator molecules have been introduced as a means to generate novel signaling patterns of muscarinic acetylcholine receptors.<sup>10,15,20</sup> Here we show for the first time that inactive muscarinic receptors correspondingly allow dualsteric binding of hybrid antagonists. For this, three series of probes were designed and synthesized. These reflect a stepwise buildup of dualsteric ligands, starting from the archetypal orthosteric antagonists atropine and scopolamine, and, for comparison, the highly potent orthosteric agonist iperoxo. Orthosteric building blocks were fused with a hexamethonium linker, which served to attach an archetypal allosteric ligand of either the phthalimide- or the naphthalimide-type. Probing test compound binding with the orthosteric radioligand [<sup>3</sup>H]N-methylscopolamine in membranes from hM<sub>2</sub>-CHO cells revealed parallel structure–binding relationships between the new antagonistic and the established dualsteric agonist hybrids. In line with this, blockade of the orthosteric site with the radioligand clearly reduced affinity of the bivalent test compounds. Sensitivity to an orthosteric receptor mutant, M<sub>2</sub> Y104A, confirmed the dualsteric binding pose of the bivalent antagonist hybrids. Regarding allosteric binding, the point mutant M<sub>2</sub> Y177Q reduced binding affinity

of atropine-derived hybrids in contrast to scopolamine derived hybrids. In line with this, atropine-derived hybrids displayed M<sub>2</sub> over M<sub>5</sub> preference in contrast to scopolamine-derived hybrids. Docking studies and molecular dynamics simulations revealed divergent orthosteric binding poses of the tropane ring system between atropine and scopolamine. As a consequence, the corresponding dualsteric ligands appear to differ with respect to both, the binding pose of the respective allosteric building blocks and the resulting subtype selectivity.

## EXPERIMENTAL SECTION

Melting points were determined on a Sanyo Gallenkamp melting point apparatus (Sanyo Gallenkamp, NL) and are uncorrected. <sup>1</sup>H NMR and <sup>13</sup>C NMR spectra were recorded with a Bruker AV 400 spectrometer (<sup>1</sup>H, 400.132 MHz; <sup>13</sup>C, 100.613 MHz). Chemical shifts ( $\delta$ ) are expressed in ppm and coupling constants ( $J$ ) in hertz. Abbreviations for data quoted are: s, singlet; d, doublet; t, triplet; m, multiplet; br, broad. The center of the peaks of CDCl<sub>3</sub> and DMSO-d<sub>6</sub> was used as internal reference. FT-IR spectra were recorded on a Bio-Rad PharmalyzIR equipped with an ATR unit. TLC analyses were performed on commercial silica gel SIL 625 UV<sub>254</sub> (Macherey-Nagel, D) sheets. The purities of new compounds were determined using capillary electrophoresis and were found to be  $\geq$ 95%. The CE analyses were performed on a Beckman Coulter P/ACE System MDQ (Fullerton, CA, USA), equipped with an UV-detector measuring at 210 nm, using a fused silica capillary (effective length 40 cm, total length 50.2 cm, diameter 50  $\mu$ m) and as a running buffer 50 mM aqueous sodium borate, pH 10.5. Prior to use, aqueous solutions were filtered through a 0.22  $\mu$ m pore-size CME (cellulose mix ester) filter (Carl Roth GmbH, Karlsruhe, Germany). The aqueous buffer was prepared using ultrapure Milli-Q water (Millipore, Milford, MA, USA).

Compounds **1**, **2**, **3**, and **4** were synthesized microwave enhanced according to ref 32 or classically according to refs 31, 32, respectively, compound 6-bromo-N,N,N-trimethyl-hexane-1-aminium bromide according to ref 44. Iper (**12**) and desmethyl-iper (**11**) were synthesized according to ref 43, and the agonist hybrids iper-6 (**13**), iper-6-phthal (**14**), and iper-6-naph (**15**) according to refs 10 and 15.

2-(3-Dimethylamino-propyl)-1,3-dihydroisoindole-1,3-dione (**1**)<sup>44</sup> yield 91%; mp 93 °C. 2-(3-Dimethylamino-2,2-dimethylpropyl)-1H-benzo[de]isoquinoline-1,3(2H)-dione (**2**): yield 90% (61%); mp 112–114 °C (112–114 °C).<sup>30</sup> 6-Bromo-N-[3-(1,3-dioxo-isoindol-2-yl)-propyl]-N,N-dimethyl-hexan-1-aminium bromide (**3**): yield 75% (63%); mp 219 °C (189–190 °C).<sup>32</sup> 6-Bromo-N-[3-(1,3-dioxo-1H-benzo[de]isoquinolin-2(3H)-yl)-2,2-dimethylpropyl]-N,N-dimethyl-hexane-1-aminium bromide (**4**): yield 70% (55%); mp 177–179 °C (178–180 °C).<sup>31</sup> 6-Bromo-N,N,N-trimethyl-hexan-1-aminium bromide: yield 75% (95%); mp 109–111 °C (106–108 °C).<sup>45</sup>

**General Procedure for the Synthesis of Allosteric/Orthosteric Hybrid Compounds (5–10).** To achieve the free scopolamine-base, the hydrobromide was dissolved in water, the pH value adjusted to 11 with 1 M aqueous sodium hydroxide solution, and finally extracted with dichloromethane. The organic phases were dried over sodium sulfate. The solvent was evaporated in vacuo to achieve the free scopolamine-base as a white viscous oil.

Atropine (2.9 g, 10 mmol) or scopolamine (3.03 g, 10 mmol), respectively, and the corresponding ammonium salt (**3**, 4.8 g; **4**, 5.5 g; **6**, 6-Bromo-N,N,N-trimethyl-hexane-1-aminium bromide, 3.0 g; 10 mmol) were dissolved in acetonitrile (20 mL) and heated to 55 °C (**10**), 85 °C (**5**, **6**, **9**), or 120 °C (**7,8**) in a sealed pressure tube. The completeness of the reactions (2–38 days) was determined by thin layer chromatography (silica gel, CH<sub>3</sub>OH/0.2 M NH<sub>4</sub>NO<sub>3</sub> 3:2,  $R_f$  = 0.6–0.7). The solutions were added dropwise to ice-cold diethyl ether. The obtained precipitate was filtered off and dried in vacuo to obtain the respective compounds.

8-[6-(N-(3-(1,3-Dioxoisoindolin-2-yl)propyl)-N,N-dimethylammonio)hexyl]-3-[(3-hydroxy-2-phenylpropanoyl)oxy]-8-methyl-8-azabicyclo[3.2.1]octan-8-iun Dibromide (**5**). Yield 48% (white solid), mp 158 °C. <sup>1</sup>H NMR (400 MHz, DMSO-d<sub>6</sub>):  $\delta$  1.29 (br, 4H), 1.65 (br, 4H), 1.87 (br, 2H), 2.10 (b, 6H), 2.63 (br, 2H),

3.00 (s, 3H), 3.05 (s, 6 H), 3.15 (br, 2H), 3.25 (br, 2H), 3.32 (m, 2H), 3.53 (ddd,  $J = J = 9.4, 5.8, 7.2$  Hz, 1H), 3.65 (m, 2H), 3.81 (dd,  $J = 5.9, 7.2$  Hz, 1H), 3.85 (br, 2H), 3.99 (ddd,  $J = 9.4, 5.8, 5.9$  Hz, 1H), 5.01 (t,  $J = 5.8$  Hz, 1H), 5.09 (t,  $J = 5.1$  Hz, 1H), 7.33 (m, 5H), 7.89 (m, 4H).  $^{13}\text{C}$  NMR (400 MHz, DMSO- $d_6$ ):  $\delta$  21.3, 21.4, 24.1, 24.3, 25.2, 25.3, 31.5, 34.5, 34.6, 49.9, 54.1, 59.8, 59.9, 60.7, 60.8, 62.9, 63.4, 64.7, 64.9, 123.1, 127.4, 128.1, 128.6, 131.7, 134.4, 136.1, 167.7, 170.2. IR [cm $^{-1}$ ]: 703, 776, 1354, 1535, 1589, 1651, 1701, 2925, 3418.

**8-[6-(N-(3-(1,3-Dioxo-1H-benzo[de]isoquinolin-2(3H)-yl)-2,2-dimethylpropyl)-N,N-dimethylammonio]hexyl]-3-[(3-hydroxy-2-phenylpropanoyl)oxy]-8-methyl-8-azabicyclo[3.2.1]octan-8-i um Dibromide (6).** Yield 60% (yellow solid); mp 169 °C.  $^1\text{H}$  NMR (400 MHz, DMSO- $d_6$ ):  $\delta$  1.24 (s, 6H), 1.34 (br, 4H), 1.63–1.90 (m, 7H), 2.08–2.29 (m, 3H), 2.52–2.62 (m, 2H), 3.08 (s, 3H), 3.20 (br, 8H), 3.33 (s, 2H), 3.45 (br, 2H), 3.50 (s, 2H), 3.69 (ddd,  $J = 9.7, 5.3, 5.4$  Hz, 1H), 3.81 (dd,  $J = 5.3, 9.1$  Hz, 1H), 3.98 (br, 2H), 3.98 (ddd,  $J = 9.7, 5.4, 9.1$  Hz, 1H), 5.02 (t,  $J = 5.4$  Hz, 1H), 5.00 (t,  $J = 5.1$  Hz, 1H), 7.25–7.40 (m, 5H), 7.90 (t,  $J = 7.7$  Hz, 2H), 8.47–8.55 (m, 4H).  $^{13}\text{C}$  NMR (101 MHz, DMSO- $d_6$ ):  $\delta$  21.4, 21.8, 24.1, 24.3, 25.3, 25.5, 31.6, 40.2, 48.8, 52.0, 54.1, 60.2, 63.0, 63.5, 64.6, 64.9, 67.0, 71.6, 122.2, 127.3, 127.4, 128.1, 128.6, 130.9, 131.3, 134.3, 136.1, 164.6, 171.2. IR [cm $^{-1}$ ]: 720, 743, 783, 930, 1028, 1163, 1234, 1339, 1588, 1658, 1702, 2947, 3055, 3388.

**9-[6-(N-(3-(1,3-Dioxoisooindolin-2-yl)propyl)-N,N-dimethylammonio]hexyl]-7-[(3-hydroxy-2-phenylpropanoyl)oxy]-9-methyl-3-oxa-9-azatricyclo[3.3.1.0 $^{2,4}$ ]nonan-9-i um Dibromide (7).** Yield 20% (light-yellow solid); mp 179 °C.  $^1\text{H}$  NMR (400 MHz, DMSO- $d_6$ ):  $\delta$  1.25 (br, 4H), 1.65 (br, 4H), 1.78 (d,  $J = 17.2$  Hz, 1H), 1.93 (d,  $J = 17.2$  Hz, 1H), 2.05 (br, 2H), 2.63 (br, 2H), 2.99 (s, 6H), 3.05 (s, 3H), 3.25 (br, 2H), 3.33 (br, 2H), 3.53 (m, 2H), 3.66 (m, 3H), 3.76 (d,  $J = 3.4$  Hz, 1H), 3.79 (m, 1H), 3.95 (m, 1H), 4.01 (d,  $J = 3.4$  Hz, 1H), 4.19 (d,  $J = 2.2$  Hz, 1H), 4.23 (d,  $J = 2.2$  Hz, 1H), 5.04 (t,  $J = 5.9$  Hz, 1H), 5.11 (br, 1H), 7.33 (m, 5H), 7.89 (m, 4H).  $^{13}\text{C}$  NMR (101 MHz, DMSO- $d_6$ ):  $\delta$  21.5, 21.6, 25.1, 25.3, 28.2, 31.8, 34.6, 44.4, 50.0, 53.5, 53.7, 54.1, 60.8, 62.1, 62.8, 62.9, 63.0, 67.6, 123.1, 127.4, 128.2, 128.5, 131.7, 134.4, 136.1, 168.0, 171.2. IR [cm $^{-1}$ ]: 720, 1038, 1396, 1534, 1652, 1710, 1769, 2988.

**9-[6-(N-(3-(1,3-Dioxo-1H-benzo[de]isoquinolin-2(3H)-yl)-2,2-dimethylpropyl)-N,N-dimethylammonio]hexyl]-7-[(3-hydroxy-2-phenylpropanoyl)oxy]-9-methyl-3-oxa-9-azatricyclo[3.3.1.0 $^{2,4}$ ]nonan-9-i um Dibromide (8).** Yield 50% (light-yellow solid); mp 212 °C.  $^1\text{H}$  NMR (400 MHz, DMSO- $d_6$ ):  $\delta$  1.30 (br, 4H), 1.36 (s, 6H), 1.73 (br, 4H), 1.79 (d,  $J = 16.9$  Hz, 1H), 1.94 (d,  $J = 16.9$  Hz, 1H), 2.65 (br, 2H), 3.09 (s, 3H), 3.17 (s, 6H), 3.39 (br, 2H), 3.55 (br, 2H), 3.64 (s, 2H), 3.69 (dd,  $J = 7.7, 8.8$  Hz, 1H), 3.77 (d,  $J = 3.3$  Hz, 1H), 4.01 (d,  $J = 3.3$  Hz, 1H), 3.80 (ddd,  $J = 9.9, 5.4, 7.7$  Hz, 1H), 3.98 (ddd,  $J = 9.9, 5.4, 8.8$  Hz, 1H), 4.15 (s, 2H), 4.20 (d,  $J = 3.3$  Hz, 1H), 4.24 (d,  $J = 3.3$  Hz, 1H), 5.04 (t,  $J = 5.9$  Hz, 1H), 5.11 (t,  $J = 5.4$  Hz, 1H), 7.35 (m, 5H), 7.91 (t,  $J = 7.5$  Hz, 2H), 8.52 (m, 4H).  $^{13}\text{C}$  NMR (101 MHz, DMSO- $d_6$ ):  $\delta$  21.7, 21.9, 25.2, 25.3, 25.5, 28.2, 44.4, 48.8, 52.0, 53.6, 53.7, 54.1, 62.1, 62.8, 62.9, 63.0, 67.0, 67.6, 71.6, 122.3, 127.3, 127.4, 127.5, 128.2, 128.5, 130.9, 131.3, 136.1, 164.7, 170.9. IR [cm $^{-1}$ ]: 777, 1236, 1335, 1589, 1649, 1700, 2943, 3410.

**3-[(Hydroxy-2-phenylpropanoyl)oxy]-8-methyl-8-[6-(N,N,N-trimethylammonio]hexyl]-8-azabicyclo[3.2.1]octan-8-i um Dibromide (9).** Yield 20% (brown solid); mp 107 °C.  $^1\text{H}$  NMR (400 MHz, DMSO- $d_6$ ):  $\delta$  1.32 (br, 4H), 1.70 (b, 3H), 1.83 (m, 2H), 2.06–2.28 (m, 3H), 2.56 (br, 2H), 3.03 (s, 3H), 3.08 (s, 9H), 3.19 (br, 2H), 3.37 (br, 2H), 3.65–3.72 (ddd,  $J = 9.8, 5.3, 9.2$  Hz, 1H), 3.81 (dd,  $J = 5.2, 9.2$  Hz, 1H), 3.85 (br, 2H), 3.98 (ddd,  $J = 9.8, 5.2, 5.3$  Hz, 1H), 5.00 (t,  $J = 5.3$  Hz, 1H), 5.10 (t,  $J = 5.3$  Hz, 1H), 7.25–7.35 (m, 5H).  $^{13}\text{C}$  NMR (101 MHz, DMSO- $d_6$ ):  $\delta$  21.3, 21.7, 24.1, 24.3, 25.2, 31.6, 40.1, 52.1, 54.1, 60.2, 62.9, 63.5, 64.6, 64.9, 65.0, 127.4, 128.0, 128.6, 136.1, 171.2. IR [cm $^{-1}$ ]: 700, 760, 974, 1346, 1480, 1628, 1716, 2868, 2953, 3400.

**7-[(3-Hydroxy-2-phenylpropanoyl)oxy]-9-methyl-9-[6-(N,N,N-trimethylammonio]hexyl]-3-oxa-9-azatricyclo[3.3.1.0 $^{2,4}$ ]nonan-9-i um Dibromide (10).** Yield 31% (light-yellow solid); mp 216–217 °C.  $^1\text{H}$  NMR (400 MHz, DMSO- $d_6$ ):  $\delta$  1.28 (br, 4H), 1.70 (br, 4H), 1.78 (d,  $J = 17.3$ , 1H), 1.93 (d,  $J = 17.1$  Hz, 1H), 2.58–2.68 (m, 2H), 3.07 (s, 12 H), 3.30 (b, 2H), 3.52–3.56 (m, 2H), 3.65–3.71 (m, 1H), 3.76

(d,  $J = 3.7$  Hz, 1H), 3.78–3.80 (m, 1H), 3.94–3.98 (m, 1H), 4.01 (d,  $J = 3.5$  Hz, 1H), 4.23 (dd,  $J = 2.2, 17.4$  Hz, 2H), 5.04 (t,  $J = 5.9$  Hz, 1H), 5.11 (t,  $J = 5.11$  Hz, 1H), 7.28–7.34 (m, 5H).  $^{13}\text{C}$  NMR (101 MHz, DMSO- $d_6$ ):  $\delta$  21.3, 21.7, 23.9, 25.3, 28.1, 28.3, 28.6, 32.1, 43.5, 52.1, 54.1, 62.7, 62.8, 62.9, 64.9, 127.3, 128.1, 128.4, 136.1, 170.8. IR [cm $^{-1}$ ]: 811, 1043, 1386, 1627, 2927

**NOESY NMR Experiments.** NOESY studies were acquired using the noesytp program on a Bruker Avance 400 MHz spectrometer, with a mixing time of 1 s. The number of scans as well as the number of dummy scans was 16. The relaxation delay was 3 s, time domain size 2048, acquisition time 0.250725 s, the transmitter frequency offset 4.603 ppm, spectral width 102091 ppm, frequency offset of the second nucleus 4.603 ppm, spectral width (F1) 102091 ppm.

**Pharmacological Experiments. Cell Culture and Membrane Preparation.** Flp-In-Chinese hamster ovary cells (Flp-In-CHO) stably expressing the hM2 receptor (CHO-hM2 cells), or the hM2 mutant receptors (CHO-hM2 Y104 $^{3,33}$ A cells; CHO-hM2 Y177 $^{EL2}$ A; CHO-hM2 Y177 $^{EL2}$ Q; CHO-hM2 Y177 $^{EL2}$ Q, T423 $^{7,36}$ H; CHO-hM2 W422 $^{7,35}$ A) and CHO-K1 cells stably expressing the hM5 receptor (CHO-K1-hM5 cells) were cultured in Ham's nutrient mixture F-12 supplemented with 10% (v/v) fetal calf serum (FCS), 100 μg mL $^{-1}$  streptomycin, 100 U mL $^{-1}$  penicillin, and 2 mM L-glutamine.

**Radioligand Binding Experiments.** Equilibrium binding and kinetic experiments using membranes of CHO-hM cells were performed in 96-well microtiter plates (ABgene, Germany) by applying a rapid filtration procedure essentially as described previously.<sup>24,29</sup>  $[^3\text{H}]$ NMS binding assays were carried out in a 10 mM HEPES, 10 mM MgCl<sub>2</sub>, 100 mM NaCl, 10 μM GDP, pH 7.4 at 30 °C.  $[^3\text{H}]$ NMS-binding was characterized by receptor densities of 1–6 pmol/mg membrane protein. Incubation times necessary to attain  $[^3\text{H}]$ NMS binding equilibrium in the presence of allosteric agents were calculated as described previously.<sup>29</sup> As an exception, Iper-6-naph (15) equilibrium data, collected with the receptor mutation M<sub>2</sub> Y104A, used, due to a low  $[^3\text{H}]$ NMS affinity, centrifugation and not rapid filtration to separate  $[^3\text{H}]$ NMS receptor complexes at the end of the respective incubation period. This separation step was carried out in silanized 1.5 mL reaction tubes at 21000g (15.300 rpm) and 15 °C for 20 min using a table centrifuge (Beckman Mikrofuge 365627, Rotor F241.5, Beckman Instruments, Palo Alto, CA). After removing the supernatant, the surface of the remaining pellet was washed once with 100 μL of incubation buffer (see above). Finally, the pellet was resuspended in 80 μL of incubation buffer and a 50 μL aliquot of the suspension dispensed into a 20 mL scintillation vial. The radioactivity contained was determined by liquid scintillation counting as described earlier.<sup>15</sup> Dissociation binding experiments were performed as two-point  $[^3\text{H}]$ NMS dissociation experiments.<sup>46</sup>

**Dynamic Mass Redistribution Measurements (DMR).** DMR assays were carried out as described earlier<sup>15,47</sup> using the beta version of the Epic device (Corning, NY, USA). Flp-In-CHO cells, Hanks' Balanced Salt Solution (HBSS), and HEPES buffer solution were obtained from Invitrogen (Carlsbad, CA, USA). In short, Flp-In-CHO cells, empty or stably transfected with the respective hM gene, were seeded in a density of 12500 cells per well in 384-well Epic microplates with 40 μL of growth medium (Ham's F-12 medium, 10% FBS, 2 mM L-glutamine, and 1% penicillin/streptomycin) and incubated for 20 h at 37 °C in an atmosphere of 5% CO until confluence was attained. After removing the cell culture medium and washing the cells twice with 50 μL of assay buffer per well (HBSS with 20 mM HEPES, pH 7.0), cells were allowed to rest in 30 μL of assay buffer in the Epic reader for 2 h at 28 °C. Following the addition of 10 μL of test compound dissolved in assay buffer, DMR responses were monitored for 1 h.

**Data Analysis.** Equilibrium binding experiments applying  $[^3\text{H}]$ NMS were analyzed using a four-parameter logistic function yielding the  $p(-\log)$  IC<sub>50</sub> and the slope factor  $n_H$  of the curve. If the observed slope factors and, successively, the bottom plateau did not differ significantly from unity and zero ( $F$  test,  $P < 0.05$ ), respectively,  $n_H$  was constrained to -1 and the bottom plateau to 0.

Homologous competition experiments were analyzed according to ref 48. For the sake of a semiquantitative comparison of  $[^3\text{H}]$ NMS

equilibrium binding collected in the presence of the hybrid compounds,  $\text{pIC}_{50}$  values were, irrespective of the slope factor of the curve, converted to apparent binding constants  $K_1$  using the Cheng–Prusoff correction. If, as with Atr-6-naph (6) in the M<sub>2</sub> Y104<sup>3,33</sup>A, the lower plateau of the [<sup>3</sup>H]NMS inhibition curve deviated significantly from “bottom plateau” = 0 (*F*-test,  $P < 0.05$ ), the true IC<sub>50</sub> (and not the inflection point) level of [<sup>3</sup>H]NMS binding inhibition was read from the curve.

Experiments in the presence of purely allosteric ligands such as W84 and Naphmethonium were analyzed according to the common allosteric ternary complex model.<sup>49</sup>

**Statistics.** Data are presented as means  $\pm$  standard error of the mean (SEM) for  $n$  observations. Comparisons of pairs were performed using unpaired two-tailed Student's *t* test. Comparison of fits were performed using the *F*-test feature built in GraphPad Prism version 5.03 for Windows, GraphPad Software, San Diego, California, USA, www.graphpad.com.  $P < 0.05$  was taken as criterion of statistical significance.

**Molecular Modeling.** All structures were docked in the M<sub>2</sub> muscarinic acetylcholine receptor crystal structure 3UON (Protein Data Bank)<sup>7</sup> using CCDCs software GOLD 5.1<sup>50–52</sup> with default settings and GOLDSCORE as scoring function. The cocrystallized inverse agonist QNB ((3R)-1-azabicyclo[2.2.2]oct-3-yl hydroxy(diphenyl)acetate) served as comparison for the orientation of atropine, scopolamine, and the orthosteric part of the hybrid-structures Atr-6-phth (5), Sco-6-phth (7), Atr-6-naph (6), and Sco-6-naph (8). The docking results and receptor interactions were analyzed with the software LigandScout<sup>53,54</sup> by building 3D-pharmacophores. Molecular dynamics simulations with Desmond 3.2<sup>55</sup> were performed with the periodic boundary conditions in the NPT ensemble and the SPC water model. The temperature and pressure were kept at 300 K and 1 atmospheric pressure. Transmembrane domains were taken from the OPM database<sup>56</sup> and were embedded in a pre-equilibrated POPC-membrane (palmitoyl-oleoyl-phosphatidyl-choline bilayer) and solvated with 0.15 M NaCl by using the system builder tool from Maestro, version 9.3, Schrödinger LLC, New York, NY, 2012. The OPLS2005 force field was used for all atoms. The docking results served as starting point for the molecular dynamics simulations. Each simulation consisted of a 6.92 ns equilibration run followed by a 20 ns production run, during which the POPC-bilayer remained stable and free from water molecules. MD results and receptor interactions were analyzed with the software VMD<sup>57</sup> and by 3D-pharmacophores using LigandScout 3.1.

## ■ ASSOCIATED CONTENT

### S Supporting Information

Information about the molecular dynamics simulations. This material is available free of charge via the Internet at <http://pubs.acs.org>.

## ■ AUTHOR INFORMATION

### Corresponding Authors

\*For U.H. (medicinal chemistry): phone, +49-931-3185460; fax, +49-931-3185494; E-mail, u.holzgrabe@pharmazie.uni-wuerzburg.de.

\*For K.M. (pharmacology): phone, +49-228-739103; fax, +49-228-739215; E-mail, k.mohr@uni-bonn.de.

### Notes

The authors declare no competing financial interest.

## ■ ACKNOWLEDGMENTS

Financial support by the Deutsche Forschungsgemeinschaft (HO1368/12-1; MO 821/2-1; KO 1582/3-2) is gratefully acknowledged.

## ■ ABBREVIATIONS USED

GPCR, G protein-coupled receptor; DMR, dynamic mass redistribution; ECD, extracellular domain; 7TM, seven transmembrane helices

## ■ REFERENCES

- (1) Lagerstrom, M. C.; Schioth, H. B. Structural diversity of G protein-coupled receptors and significance for drug discovery. *Nature Rev. Drug Discovery* **2008**, *7*, 339–357.
- (2) Rasmussen, S. G. F.; Choi, H.-J.; Rosenbaum, D. M.; Kobilka, T. S.; Thian, F. S.; Edwards, P. C.; Burghammer, M.; Ratnala, V. R. P.; Sanishvili, R.; Fischetti, R. F.; Schertler, G. F. X.; Weis, W. I.; Kobilka, B. K. Crystal structure of the human  $\beta 2$  adrenergic G-protein-coupled receptor. *Nature* **2007**, *450*, 383–387.
- (3) Jaakola, V. P.; Griffith, M. T.; Hanson, M. A.; Cherezov, V.; Chien, E. Y.; Lane, J. R.; Ijzerman, A. P.; Stevens, R. C. The 2.6 angstrom crystal structure of a human A2A adenosine receptor bound to an antagonist. *Science* **2008**, *322* (5905), 1211–1217.
- (4) Chien, E. Y.; Liu, W.; Zhao, Q.; Katritch, V.; Han, G. W.; Hanson, M. A.; Shi, L.; Newman, A. H.; Javitch, J. A.; Cherezov, V.; Stevens, R. C. Structure of the human dopamine D3 receptor in complex with a D2/D3 selective antagonist. *Science* **2010**, *330* (6007), 1091–1095.
- (5) Rasmussen, S. G.; Choi, H. J.; Fung, J. J.; Pardon, E.; Casarosa, P.; Chae, P. S.; Devree, B. T.; Rosenbaum, D. M.; Thian, F. S.; Kobilka, T. S.; Schnapp, A.; Konetzki, I.; Sunahara, R. K.; Gellman, S. H.; Pautsch, A.; Steyaert, J.; Weis, W. I.; Kobilka, B. K. Structure of a nanobody-stabilized active state of the beta(2) adrenoceptor. *Nature* **2011**, *469* (7329), 175–180.
- (6) Shimamura, T.; Shiroishi, M.; Weyand, S.; Tsujimoto, H.; Winter, G.; Katritch, V.; Abagyan, R.; Cherezov, V.; Liu, W.; Han, G. W.; Kobayashi, T.; Stevens, R. C.; Iwata, S. Structure of the human histamine H1 receptor complex with doxepin. *Nature* **2011**, *475* (7354), 65–70.
- (7) Haga, K.; Kruse, A. C.; Asada, H.; Yurugi-Kobayashi, T.; Shiroishi, M.; Zhang, C.; Weis, W. I.; Okada, T.; Kobilka, B. K.; Haga, T.; Kobayashi, T. Structure of the human M2 muscarinic acetylcholine receptor bound to an antagonist. *Nature* **2012**, *482*, 547–551.
- (8) Kruse, A. C.; Ring, A. M.; Manglik, A.; Hu, J.; Hu, K.; Eitel, K.; Hübner, H.; Pardon, E.; Valant, C.; Sexton, P. M.; Christopoulos, A.; Felder, C. C.; Gmeiner, P.; Steyaert, J.; Weis, W. I.; Garcia, K. C.; Wess, J.; Kobilka, B. K. Activation and allosteric modulation of a muscarinic acetylcholine receptor. *Nature* **2013**, *504*, 101–106.
- (9) Kruse, A. C.; Hu, J.; Pan, A. C.; Arlow, D. H.; Rosenbaum, D. M.; Rosemond, E.; Green, H. F.; Liu, T.; Chae, P. S.; Dror, R. O.; Shaw, D. E.; Weis, W. I.; Wess, J.; Kobilka, B. K. Structure and dynamics of the M<sub>3</sub> muscarinic acetylcholine receptor. *Nature* **2012**, *482*, 552–556.
- (10) Bock, A.; Merten, N.; Schrage, R.; Dallanoce, C.; Bätz, J.; Klöckner, J.; Schmitz, J.; Matera, C.; Simon, K.; Kebig, A.; Peters, L.; Müller, A.; Schrobang-Ley, J.; Tränkle, C.; Hoffmann, C.; De Amici, M.; Holzgrabe, U.; Kostenis, E.; Mohr, K. The allosteric vestibule of a seven transmembrane helical receptor controls G-protein coupling. *Nature Commun.* **2012**, *3*, 1044 DOI: 10.1038/ncomms2028.
- (11) Katritch, V.; Cherezov, V.; Stevens, R. C. Diversity and modularity of G protein-coupled receptor structures. *Trends Pharmacol. Sci.* **2012**, *33*, 17–27.
- (12) Dror, R. O.; Pan, A. C.; Arlow, D. H.; Borhani, D. W.; Maragakis, P.; Shan, Y.; Xu, H.; Shaw, D. E. Pathway and mechanism of drug binding to G-protein-coupled receptors. *Proc. Natl. Acad. Sci. U. S. A.* **2011**, *108* (32), 13118–13123.
- (13) Mohr, K.; Schmitz, J.; Schrage, R.; Tränkle, C.; Holzgrabe, U. Molecular Alliance: from orthosteric to allosteric ligands to dualistic/bitopic agonists at G-protein coupled receptors. *Angew. Chem., Int. Ed.* **2013**, *52* (2), 508–516.
- (14) Disingrini, T.; Muth, M.; Dallanoce, C.; Barocelli, E.; Bertoni, S.; Kellershohn, K.; Mohr, K.; De Amici, M.; Holzgrabe, U. Design, Synthesis, and Action of Oxotremorine-Related Hybrid-Type Allos-

- teric Modulators of Muscarinic Acetylcholine Receptors. *J. Med. Chem.* **2006**, *49* (1), 366–372.
- (15) Antony, J.; Kellershohn, K.; Mohr-Andrä, M.; Kebig, A.; Prilla, S.; Muth, M.; Heller, E.; Disingrini, T.; Dallanoce, C.; Bertoni, S.; Schrobang, J.; Tränkle, C.; Kostenis, E.; Christopoulos, A.; Höltje, H. D.; Barocelli, E.; De Amici, M.; Holzgrabe, U.; Mohr, K. Dualsteric GPCR targeting: a novel route to binding and signaling pathway selectivity. *FASEB J.* **2009**, *23*, 442–450.
- (16) Schrage, R.; Seemann, W. K.; Klöckner, J.; Dallanoce, C.; Racké, K.; Kostenis, E.; De Amici, M.; Holzgrabe, U.; Mohr, K. Agonists with supraphysiological efficacy at the muscarinic M2 ACh receptor. *Br. J. Pharmacol.* **2013**, *169*, 357–370.
- (17) Dallanoce, C.; Conti, P.; De Amici, M.; De Micheli, C.; Barocelli, E.; Chiavarini, M.; Ballabeni, V.; Bertoni, S.; Impicciatore, M. Synthesis and functional characterization of novel derivatives related to oxotremorine and oxotremorine-M. *Bioorg. Med. Chem.* **1999**, *7*, 1539–1547.
- (18) Barocelli, E.; Ballabeni, V.; Bertoni, S.; Dallanoce, C.; De Amici, M.; De Micheli, C.; Impicciatore, M. New analogues of oxotremorine and oxotremorine-M: estimation of their in vitro affinity and efficacy at muscarinic receptor subtypes. *Life Sci.* **2000**, *67* (6), 717–723.
- (19) Matera, C.; Flammini, L.; Quadri, M.; Vivo, V.; Ballabeni, V.; Holzgrabe, U.; Mohr, K.; De Amici, M.; Barocelli, E.; Bertoni, S.; Dallanoce, C. Bis(ammonio)alkane-type agonists of muscarinic acetylcholine receptors: synthesis, in vitro functional characterization, and in vivo evaluation of their analgesic activity. *Eur. J. Med. Chem.* **2014**, *75*, 222–232.
- (20) Valant, C.; Gregory, K. J.; Hall, N. E.; Scammells, P. J.; Lew, M. J.; Sexton, P. M.; Christopoulos, A. A novel mechanism of G protein-coupled receptor functional selectivity. Muscarinic partial agonist McNA-343 as a bitopic orthosteric/allosteric ligand. *J. Biol. Chem.* **2008**, *283* (43), 29312–29321.
- (21) Tahtaoui, C.; Parrot, I.; Klotz, P.; Guillier, F.; Galzi, J. L.; Hibert, M.; Ilien, B. Fluorescent pirenzepine derivatives as potential bitopic ligands of the human M1 muscarinic receptor. *J. Med. Chem.* **2004**, *47*, 4300–4315.
- (22) Daval, S. B.; Valant, C.; Bonnet, D.; Kellenberger, E.; Hibert, M.; Galzi, J. L.; Ilien, B. Fluorescent derivatives of AC-42 to probe bitopic orthosteric/allosteric binding mechanisms on muscarinic M1 receptors. *J. Med. Chem.* **2012**, *55*, 2125–2143.
- (23) Decker, M.; Holzgrabe, U. M1Muscarinic Acetylcholine Receptor Allosteric Modulators as Potential Therapeutic Opportunities for Treating Alzheimer's Disease. *Med. Chem. Commun.* **2012**, *3*, 752–762.
- (24) Bock, A.; Chirinda, B.; Krebs, F.; Messerer, R.; Bätz, J.; Muth, M.; Dallanoce, C.; Klingenthal, D.; Tränkle, C.; Hoffmann, C.; De Amici, M.; Holzgrabe, U.; Kostenis, E.; Mohr, K. Dynamic ligand binding dictates partial agonism at a G protein-coupled receptor. *Nature Chem. Biol.* **2014**, *10*, 18–20.
- (25) Luellmann, H.; Ohnesorge, F. K.; Schauwecker, G. C.; Wassermann, O. Inhibition of the actions of carbachol and DFP on guinea pig isolated atria by alkane-bis-ammonium compounds. *Eur. J. Pharmacol.* **1969**, *6*, 241–247.
- (26) Clark, A. L.; Mitchelson, F. The inhibitory effect of gallamine on muscarinic receptors. *Br. J. Pharmacol.* **1976**, *58*, 323–331.
- (27) Stockton, J. M.; Birdsall, N. J. M.; Burgen, A. S. V.; Hulme, E. C. Modification of the binding properties of muscarinic receptors by gallamine. *Mol. Pharmacol.* **1983**, *23*, 551–557.
- (28) Voigtlander, U.; Mohr, M.; Raasch, A.; Tränkle, C.; Buller, S.; Ellis, J.; Höltje, H. D.; Mohr, K. Allosteric site on muscarinic acetylcholine receptors: identification of two amino acids in the muscarinic M2 receptor that account entirely for the M2/MS subtype selectivities of some structurally diverse allosteric ligands in *N*-methylscopolamine-occupied receptors. *Mol. Pharmacol.* **2003**, *64*, 21–31.
- (29) Prilla, S.; Schrobang, J.; Ellis, J.; Höltje, H. D.; Mohr, K. Allosteric interactions with muscarinic acetylcholine receptors: complex role of the conserved tryptophan M2422Trp in a critical cluster of amino acids for baseline affinity, subtype selectivity, and cooperativity. *Mol. Pharmacol.* **2006**, *70* (1), 181–193.
- (30) Muth, M.; Bender, W.; Scharfenstein, O.; Holzgrabe, U.; Balatkova, E.; Tränkle, C.; Mohr, K. Systematic development of high affinity bis(ammonio)alkane-type allosteric enhancers of muscarinic ligand binding. *J. Med. Chem.* **2003**, *46*, 1031–1040.
- (31) Muth, M.; Sennwitz, M.; Mohr, K.; Holzgrabe, U. Muscarinic allosteric enhancers of ligand binding: pivotal pharmacophoric elements in hexamethonio-type agents. *J. Med. Chem.* **2005**, *48*, 2212–2217.
- (32) Schmitz, J.; Heller, E.; Holzgrabe, U. A fast and efficient track to allosteric modulators of muscarinic receptors: microwave-assisted synthesis. *Monatsh. Chem.* **2007**, *138*, 171–174.
- (33) Glaser, R.; Peng, Q.-J.; Perlin, A. S. Stereochemistry of the methyl group in salts of tropane alkaloids. *J. Org. Chem.* **1988**, *53*, 2172–80.
- (34) Schneider, H. J.; Stürm, L. Carbon-13 NMR spectroscopic and stereochemical investigations. 13. Conformations and nitrogen inversion barriers in tropane compounds. *Angew. Chem.* **1976**, *88* (17), 574–575.
- (35) Schröter, A.; Tränkle, C.; Mohr, K. Modes of allosteric interactions with free and [<sup>3</sup>H]N-methylscopolamine-occupied muscarinic M2 receptors as deduced from buffer-dependent potency shifts. *Naunyn Schmiedeberg's Arch. Pharmacol.* **2000**, *362*, 512–519.
- (36) Jäger, D.; Schmalenbach, C.; Prilla, S.; Schrobang, J.; Kebig, A.; Sennwitz, M.; Heller, E.; Tränkle, C.; Holzgrabe, U.; Höltje, H. D.; Mohr, K. Allosteric small molecules unveil a role of an extracellular E2/transmembrane helix 7 junction for G protein-coupled receptor activation. *J. Biol. Chem.* **2007**, *282*, 34968–34976.
- (37) de Amici, M.; Dallanoce, C.; Holzgrabe, U.; Tränkle, C.; Mohr, K. Allosteric Ligands for G protein-coupled receptors: a novel strategy with attractive therapeutic opportunities. *Med. Res. Rev.* **2010**, *30*, 463–549.
- (38) Bock, A.; Mohr, K. Dualsteric GPCR targeting and functional selectivity: the paradigmatic M(2) muscarinic acetylcholine receptor. *Drug Discovery Today Technol.* **2013**, *10*, e245–e252.
- (39) Valant, C.; Robert Lane, J.; Sexton, P. M.; Christopoulos, A. The best of both worlds? Bitopic orthosteric/allosteric ligands of g protein-coupled receptors. *Annu. Rev. Pharmacol. Toxicol.* **2012**, *52*, 153–178.
- (40) Ballesteros, J. A.; Weinstein, H. Integrated methods for the construction of three-dimensional models and computational probing of structure-function relationships in G protein-coupled receptors. *Methods Neurosci.* **1995**, *25*, 366–428.
- (41) Ellis, J.; Huyler, J. H.; Brann, M. R. Allosteric regulation of cloned m1–m5. muscarinic receptor subtypes. *Biochem. Pharmacol.* **1991**, *42*, 1927–1932.
- (42) Buller, S.; Zlotos, D. P.; Mohr, K.; Ellis, J. Allosteric site on muscarinic acetylcholine receptors: a single amino acid in transmembrane region 7 is critical to the subtype selectivities of caracurine V derivatives and alkane-bisammonium ligands. *Mol. Pharmacol.* **2002**, *61*, 160–168.
- (43) Kloeckner, J.; Schmitz, J.; Holzgrabe, U. Convergent, short synthesis of the muscarinic superagonist. *Tetrahedron Lett.* **2010**, *51*, 3470–3472.
- (44) Raasch, A.; Scharfenstein, O.; Tränkle, C.; Holzgrabe, U.; Mohr, K. Elevation of ligand binding to muscarinic M2 acetylcholine receptors by bis(ammonio)alkane-type allosteric modulators. *J. Med. Chem.* **2002**, *45*, 3809–3812.
- (45) Gray, A. P.; Schlieper, D. C.; Spinner, E. E.; Cavallito, C. J. The preparation of some omega-bromoalkyl quaternary ammonium salts. *J. Am. Chem. Soc.* **1955**, *77*, 3648–3649.
- (46) Kostenis, E.; Mohr, K. Two-point kinetic experiments to quantify allosteric effects on radioligand dissociation. *Trends Pharmacol. Sci.* **1996**, *17*, 280–283.
- (47) Schröder, R.; Schmidt, J.; Blättermann, S.; Peters, L.; Janssen, N.; Grundmann, M.; Seemann, W.; Kaufel, D.; Merten, N.; Drewke, C.; Gomeza, J.; Milligan, G.; Mohr, K.; Kostenis, E. Applying label-free dynamic mass redistribution technology to frame signaling of G

protein-coupled receptors noninvasively in living cells. *Nature Protoc.* **2011**, *6*, 1748–1760.

(48) DeBlasi, A.; O'Reilly, K.; Motulsky, H. J. Calculating receptor number from binding experiments using same compound as radioligand and competitor. *Trends Pharmacol. Sci.* **1989**, *10*, 227–229.

(49) Ehlert, F. J. Estimation of the affinities of allosteric ligands using radioligand binding and pharmacological null methods. *Mol. Pharmacol.* **1988**, *33*, 187–194.

(50) Jones, G.; Willett, P.; Glen, R. C. Molecular recognition of receptor sites using a genetic algorithm with a description of desolvation. *J. Mol. Biol.* **1995**, *245*, 43–53.

(51) Jones, G.; Willett, P.; Glen, R. C.; Leach, A. R.; Taylor, R. Development and validation of a genetic algorithm for flexible docking. *J. Mol. Biol.* **1997**, *267*, 727–748.

(52) Verdonk, M. L.; Cole, J. C.; Hartshorn, M. J.; Murray, C. W.; Taylor, R. D. Improved protein–ligand docking using GOLD. *Proteins: Struct., Funct., Genet.* **2003**, *52*, 609–623.

(53) Wolber, G.; Dornhofer, A. A.; Langer, T. Efficient overlay of small organic molecules using 3D pharmacophores. *J. Comput.-Aided Mol. Des.* **2006**, *20*, 773–788.

(54) Wolber, G.; Langer, T. LigandScout: 3-d pharmacophores derived from protein-bound ligands and their use as virtual screening filters. *J. Chem. Inf. Model.* **2005**, *45*, 160–169.

(55) Bowers, K. J.; Chow, E.; Huageng, X.; Dror, R. O.; Eastwood, M. P.; Gregersen, B. A.; Klepeis, J. L.; Kolossvary, I.; Moraes, M. A.; Sacerdoti, F. D.; Salmon, J. K.; Yibing, S.; Shaw, D. E. In *Scalable Algorithms for Molecular Dynamics Simulations on Commodity Clusters*. SC 2006 Conference, Proceedings of the ACM/IEEE, Tampa, FL, November 11–17, 2006, pp 43–43.

(56) Lomize, M. A.; Pogozheva, I. D.; Mosberg, H. I. OPM: Orientations of proteins in membranes database. *Bioinformatics* **2006**, *22*, 623–625.

(57) Humphrey, W.; Dalke, A.; Schulten, K. VMD: Visual molecular dynamics. *J. Mol. Graphics Modell.* **1996**, *14*, 33–38.